ENERGY ABSORPTION IN THERMOPLASTICALLY STAMPED COMPOSITE GRID STRUCTURES

Changsheng Gan, Ronald F. Gibson and Golam M. Newaz
Mechanical Engineering Department, Advanced Composites Research Laboratory
Wayne State University, Detroit, MI 48202

Abstract

This paper summarizes results from an analytical/experimental study of the energy absorption characteristics of grid-stiffened composite structures under transverse loading. Tests and finite element simulations were carried out for quasi-static loading of isogrid E-glass/polypropylene panels in 3-point bending. Test panels were fabricated by using a thermoplastic stamping process and co-mingled E-glass/polypropylene yarns. The results of the tests and simulations show that these types of structures have excellent energy absorption characteristics, and that most of the energy absorption occurs beyond initial failure. Results for isogrid panels loaded on the skin side will be compared with similar results for loading on the rib side, and conclusions regarding design of such structures for energy absorption will be offered.

Background

Geodesic grid structures have a long and illustrious history, including the famous geodesic domes of Buckminster Fuller and the damage tolerant Wellington bombers of World War II (1). These early grid structures typically consisted of wood or metal grid frames and fabric skins, but in recent years it has been found that grids consisting of unidirectional composite ribs can be used to great advantage (2-4). So far, the use of grid-stiffened composite structures has been mainly restricted to relatively high cost, low volume aerospace applications such as launch vehicles (5) and orbital satellites (6), but there appears to be considerable potential for their use in low cost, high volume applications such as automotive vehicles and civil infrastructure. Thermoplastic stamping has been shown to be a fast and effective means of fabricating low cost composite grid structures (7). Good impact energy absorption is a requirement in many of these potential applications such as door and floor panels in automotive vehicle structures and bridge decks in civil infrastructure. The objective of the current research is to fabricate composite grid panels using a low cost thermoplastic stamping process and to evaluate their energy absorption characteristics under transverse loading using both 3-point bending tests and finite element simulations.

Experiments

Specimen Materials and Fabrication

Isogrid panel specimens with ribs oriented at angles of $0^o \pm 60^o$ were fabricated by thermoplastic stamping in a specially grooved steel mold (Fig. 1) following the procedure outlined by Goldsworthy and Hiel (7).

Figure 1. Isogrid panel specimen and mold.

Overall panel dimensions were 304 mm x 264 mm, the rib cross-sectional dimensions were 6.36 mm x 6.36 mm and the skin thickness was 1.28 mm. The composite material used was Vetrotex Twintex© E-glass/polypropylene (PP), which consists of co-mingled E-glass reinforcing fibers and polypropylene matrix fibers. The ribs in the grids were made of unidirectional Twintex ©E-glass/PP roving and the skins were made of woven Twintex © E-glass/PP. The co-mingled unidirectional E-glass/PP fibers were hand laid-up into grooves of the steel mold to form the ribs of the isogrid patterns, then four layers of woven fabric Twintex© were layered on top of the ribs to form the skin. The mold with the composite layup was then placed in a TMP Composite Vacuum Press and molded under vacuum at 415F for 10 minutes with 65 psi mold pressure and 5 minutes with 195 psi mold pressure, then cooled to room temperature at 195 psi pressure, then the vacuum was released. The fiber volume fractions in all ribs were controlled by counting the number of rovings in each groove and

using the same number for all samples. Since it is very difficult to lay-up enough roving in the grooves to keep the fiber volume fraction of the ribs at a reasonable level in a one step process, a multiple step fabrication procedure was used. First, ten pieces of roving were laid into every groove of the steel mold and then molded to form an isogrid or square grid. Second, the resulting grid was removed from the mold and another ten pieces of rovings were wound into each groove of the mold, then the previously molded grid was placed on the top and the new grid was molded. A new isogrid with higher fiber volume fraction was thus fabricated. By repeating the above steps three times, the desired fiber volume fraction of 0.45 was obtained. The four layer balanced woven fabrics of the same materials were co-molded to form an isogrid stiffened plate specimen.

3-Point Bending Tests

As shown in Fig. 2, the isogrid panel specimens were loaded in 3-point bending in a Enduratec SmartTest servopneumatic testing machine operating in displacement control at a rate of 0.05 mm/s.

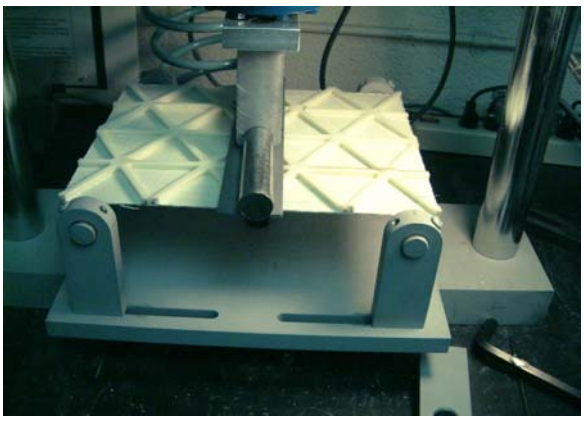

Figure 2. Test setup for 3-point bending.

The support span was 255 mm and a transverse line load was applied at midspan with a steel bar loading fixture. Energy absorption was characterized by plotting load-displacement curves and calculating the specific energy absorption (SEA) as the nonrecoverable area under the load-displacement curve beyond initial failure divided by the loaded mass of the specimen between the supports. Failure modes associated with various features of the load-displacement curves were observed and recorded during the tests. In separate experiments, loading was applied on the rib side and on the skin side for comparison of energy absorption and associated failure modes.

Finite Element Simulations

For comparison with experimental results, numerical simulations were generated by using HYPERMESH for mesh generation and ABAQUS for the finite element analysis. 3-D solid elements (type C3D8) were used to model the ribs and 2-D shell elements (type S4) were used to model the skin. A typical finite element model having 2832 elements is shown in Fig. 3.

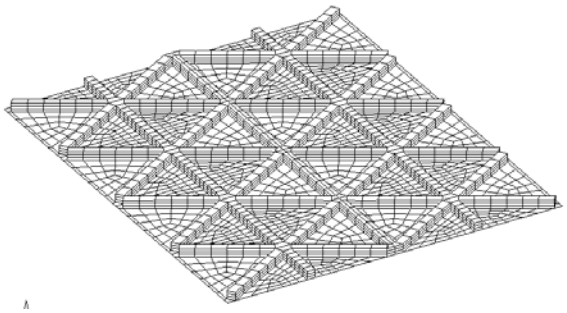

Figure 3. Finite element model of isogrid panel.

Elastic constants of the unidirectional rib material were estimated by using micromechanics models, while those of the woven skin were provided by Vetrotex. Longitudinal tensile and compressive strengths of the unidirectional rib material were found from 3-point bending tests of unidirectional beams similar to the ribs, while the corresponding transverse strengths were estimated from micromechanics. Strengths of the woven skin material were provided by Vetrotex.

A FORTRAN subroutine was implemented within the ABAQUS code to incorporate the material failure models. The user subroutine picks up the stress components of each element for each increment, and substitutes them into the appropriate failure criterion. The Maximum Stress Criterion was used for 3-D solid ribs and the combined stress criterion based on Chang-Lessard model was used for the skin. If no damage has been found, the program proceeds to a new load step. However, if any failure is detected, the program iterates the current solution with the degraded properties until the nonlinear equations of equilibrium are satisfied. An exponential decay rule was used to insure convergence following initial and subsequent failures. The degradation rate parameter affects damage front propagation within the material. The rate at which the material degrades determines the propagation of the damage front and therefore the spreading of the load to the surrounding material. Further details on the finite element simulations can be found in the dissertation by Gan (8).

Results and Comparisons

Figure 4 shows a typical comparison of experimental load-displacement results for the isogrid panel loaded on the rib side with corresponding results for loading on the skin side, while Figure 5 shows a comparison

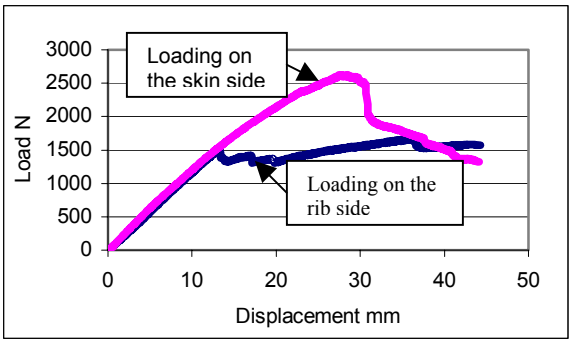

Figure 4. Comparison of measured load-displacement curves for isogrid panel loaded on rib side with corresponding results for loading on the skin side.

of predicted and measured results for the same isogrid panel. The maximum displacement of about 43 mm was limited by the test apparatus and complete failure of the specimens was not observed.

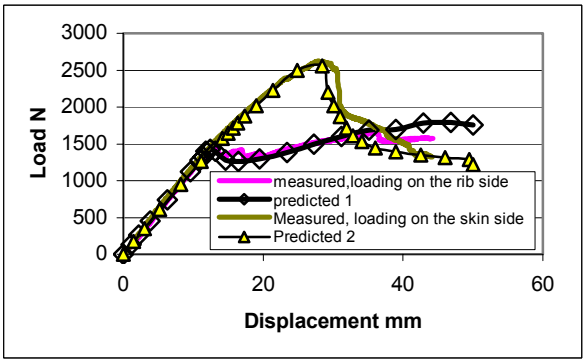

Figure 5. Predicted and measured responses for isogrid panel loaded on the rib side or skin side .

It is seen that the behavior beyond initial failure is quite different for the two loading conditions. For loading on the rib side, sequential local compressive failures of ribs by microbuckling led to a series of relatively small load drops. However, for loading on the skin side, local tensile failures (fiber breakage) in the ribs and skin buckling led to a substantial load drop following the peak load. The specific energy absorption values for the two cases are compared in Figure 6, where it is seen that the SEA for the case of

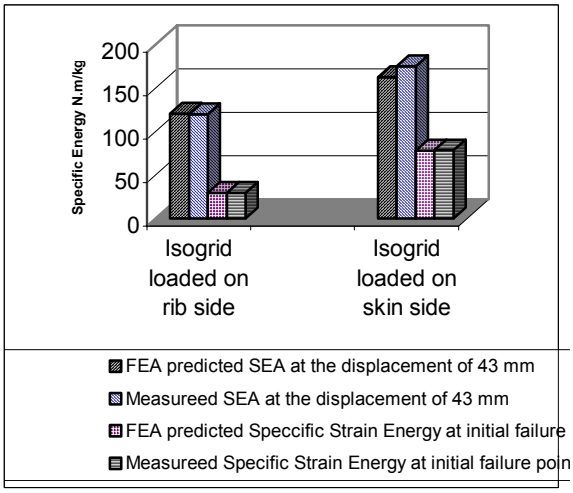

Figure 6. Comparison of predicted and measured energy absorption for isogrid panels loaded on rib side and skin side.

loading on the skin side is higher than that of loading on the rib side. It it is important to remember, however, that the SEA corresponding to complete failure is unknown in both cases, and the load following initial failure seems to remain at a reasonably constant level and even increases slightly for the case loading on the rib side, whereas the load is trending downward following a sharp load drop after initial failure for loading on the skin side. So it is believed that the SEA at final failure will be larger for loading on the rib side than for loading on the skin side. Predicted and measured values of the specific strain energy at initial failure are also given in Fig. 6, and the agreement between predicted and measured values is seen to be reasonable for both SEA and specific strain energy. Additional results for square grid structures and sandwich structures may be found in the dissertation by Gan (8). For example, unlike the grid structures, foam core sandwich structures of similar size under similar transverse loading were observed to exhibit catastrophic failures and corresponding sharp load drops without development of a stable progressive damage process.

Concluding Remarks

Transverse load-displacement relationships and the corresponding energy absorption characteristics of thermoplastically stamped E-glass/polypropylene composite isogrid structures have been studied using both quasi-static 3-point bending tests and corresponding finite element simulations. Due to displacement limitations of the test apparatus, it was not possible to achieve complete failure of the test specimens, but observations within the limited

displacement range led to some important conclusions. When transverse loading is applied on the rib side, once the peak load is achieved a stable damage progression process develops, and this process consists of a sequence of relatively small load drops (and in some cases, slight increases in the load) corresponding to local compressive microbuckling of the ribs. When the transverse loading is applied on the skin side, however, the load drop after the peak load is much larger, and the load continues to drop due to the lack of a stable damage progression process. Although the SEA based on the 43 mm maximum displacement was greater for loading on the skin side, it is believed that if complete failure can be achieved, the maximum SEA will occur for loading on the rib side. Finite element simulations of progressively damaged isogrids show reasonable agreement with experiments.

Acknowledgements

The authors gratefully acknowledge the support of the Wayne State University Institute for Manufacturing Research.

References

1. Rehfield, L. W., "A Brief History of Analysis Methodology for Grid-stiffened Geodesic Composite Structures," *Proc. 44th Intl. SAMPE Symposium*, on CD-ROM (1999).
2. Chen, H., and Tsai, S. W., "Analysis and Optimum Design of Composite Grid Structures", *Journal of Composite Materials*, 30:4, 503-534 (1996).
3. Huybrechts, S. and Tsai, S.W. , " Analysis and Behavior of Grid Structures", *Composite Science and Technology* , 56:9, 1001-1015 (1996).
4. Chen,Y. and Gibson, R.F. , "Analytical and Experimental Studies of Composite Isogrid Structures with Internal Passive Damping", *Mechanics of Advanced Materials and Structures* , 10:2, 127-143 (2003).
5. Wegner, P. M., and Higgins, J. E., "Compressive Response of Grid-stiffened Structures Having Thin Face Sheets," *Proc. Tenth U.S.-Japan Conference on Composite Materials*, F. K. Chang, Editor, 925-930 (2002).
6. Hahn, S. E., and Ozaki, T., "Thermal and Structural Requirements for Grid-stiffened Satellite Structures," *Proc. Tenth U.S.-Japan Conference on Composite Materials*, F. K. Chang, Editor, 909-916 (2002).
7. Goldsworthy, W. B., and Hiel, C., "Thermoplastics Technology Applied to Manufacturing of Grid-stiffened Structures," *Proc. 44th Intl. SAMPE Symposium*, on CD-ROM (1999).
8. Gan. C., *Behavior of Grid-stiffened Composite Structures Under Transverse Loading*, Ph.D. Dissertation, Wayne State University (2003).